

Heteroepitaxy of flexible piezoelectric Pb(Zr_{0.53}Ti_{0.47})O₃ sensor on inorganic mica substrate for lamb wave-based structural health monitoring



Xiyuan Zhang^{a,b,1}, Yu Wang^{c,1}, Xinnna Shi^{a,b}, Jie Jian^d, Xuejing Wang^d, Min Li^{a,b}, Yanda Ji^{a,b}, Fengjiao Qian^{a,b}, Jiyu Fan^{a,b}, Haiyan Wang^d, Lei Qiu^{c,***}, Weiwei Li^{a,b,e,***}, Hao Yang^{a,b,*}

^a College of Science, Nanjing University of Aeronautics and Astronautics, Nanjing, 211106, China

^b MIIT Key Laboratory of Aerospace Information Materials and Physics, Nanjing University of Aeronautics and Astronautics, Nanjing, 211106, China

^c Research Center of Structural Health Monitoring and Prognosis, State Key Laboratory of Mechanical Structures, Nanjing University of Aeronautics and Astronautics, Nanjing, 211106, China

^d School of Materials Engineering, Purdue University, West Lafayette, IN, 47907, USA

^e Department of Materials Science & Metallurgy, University of Cambridge, 27 Charles Babbage Road, Cambridge, CB3 0FS, UK

ARTICLE INFO

Keywords:

Flexible sensor

Piezoelectric sensor

PZT

Lamb wave

Structural health monitoring

ABSTRACT

Active Lamb wave detection is an effective and simple monitoring method for structural health monitoring (SHM). Piezoelectric lead zirconate titanate (PZT) ceramics are most commonly used as transducers to excite and receive Lamb wave. However, due to their hardness, thickness and brittleness, PZT ceramics are severely limited in detecting damage on curved surface structures. Herein, we report that flexible PZT film sensor is an excellent candidate for receiving Lamb wave used in Lamb wave-based SHM of aircraft. An improved piezoelectric coefficient d_{33} ($\sim 130 \text{ pm V}^{-1}$) is obtained in epitaxial PZT films grown on flexible inorganic mica substrates via van der Waals heteroepitaxy. Superior stable ferroelectricity and piezoelectricity retain in flexible PZT film after bending 10^4 cycles under a radius of 8 mm. As proven by experiment and simulation, flexible PZT film is demonstrated as an ultrasonic sensor with high sensitivity to be bonded on the curved aluminum plate for Lamb wave-based damage monitoring. Our work demonstrates that flexible PZT films have enormous potential for *real-time* light-weight and high-sensitivity receiver sensors for the SHM of aging aircraft.

1. Introduction

The structural health monitoring (SHM) of aircraft [1–5] has drawn extensive attention because it can monitor and evaluate the structural status, lengthen the maintenance intervals, reduce the life-cycle costs, improve the reliability and safety of aircraft and realize the condition-based maintenance (CBM) in *real-time*. It can acquire information related to the structural status in *real-time* through the advanced sensor network integrated in the aircraft structures. Through combining the advanced information processing methods with modeling methods, the structural characteristic parameters can be extracted and structural damage and other information can be identified. Conventional non-destructive testing (NDT) methods, such as ultrasonic [6], infrared thermography (IRT) [7], x-radiographic detection [8] and teraHertz

imaging [9] are available for detecting fatigue damage, hidden cracks or corrosion of aircraft structures without compromising the structural integrity. However, these methods are external, relatively expensive and require heavy instruments and human interference, which pose obstacles in using at a *real-time* SHM.

Among the existing SHM methods (Table S1), Lamb wave-based SHM [10–14] has attracted huge attention. It is widely adopted to detect damage in plate-like structures used in aircraft owing to their ability to propagate long distances with minimal attenuation, omnidirectional dissemination and high sensitivity to small imperfections. Also, it can quantitatively evaluate damage that is greater than 1/4 of its wavelength. The information about damages is monitored by changes in characteristics of an elastic wave via its interaction with damage, which is recorded by transducers. To generate and receive Lamb wave, various

* Corresponding author. College of Science, Nanjing University of Aeronautics and Astronautics, Nanjing, 211106, China.

** Corresponding author.

*** Corresponding author. College of Science, Nanjing University of Aeronautics and Astronautics, Nanjing, 211106, China.

E-mail addresses: lei.qiu@nuaa.edu.cn (L. Qiu), w1337@cam.ac.uk (W. Li), yanghao@nuaa.edu.cn (H. Yang).

¹ Xiyuan Zhang and Yu Wang contributed equally to this work.

transducers, such as air-coupled transducer, wedge transducer, electromagnetic acoustic transducer, piezoelectric wafers or ceramics and laser transducer, have been investigated. One of the most commonly used Lamb wave transducers is lead zirconate titanate ($\text{PbZr}_{1-x}\text{Ti}_x\text{O}_3$, PZT) ceramic because of its prominent piezoelectric property and high ferroelectric Curie temperature [11,12]. However, the fixed dimension, rigidity and brittleness of PZT ceramics greatly limit their application in SHM of complex components with curved surfaces. Moreover, for the SHM of large-area aircraft structures, the additional weight brought by PZT ceramics is also a problem that cannot be ignored. In addition, the relatively large thickness of PZT ceramics also limits their integration into polymer-matrix composite structures during the manufacturing process [15]. Therefore, it is of great significance to develop a flexible and light-weight piezoelectric transducer.

To overcome the limitations of PZT ceramics, organic piezoelectric polymer sensor like polyvinylidene fluoride (PVDF) which is light in weight and thin in depth bonded on specimen was used in Lamb wave-based SHM [16–18]. However, the performance of piezoelectric properties reported in PVDF is not ideal and the interdigital electrode pattern in the PVDF could affect the interpretation of Lamb wave signals [19]. In addition, the poor thermal stability of PVDF limits its high temperature applications.

Flexible oxide piezoelectric films open a new pathway for non-destructive inspection sensors. To achieve the coupling of piezoelectricity and mechanical stretchability, a complex process has been used to transfer oxide piezoelectric films to flexible organic polymer substrates and metal foils [20–22]. However, there are significant challenges to attain good performance due to some intrinsic limitations of organic polymer substrates and metal foils [23–26] such as significant attenuation of Lamb wave energies, large mismatch crystal structures and thermal expansion coefficients, etc. Besides, this method fails to overcome the high temperature intolerance of organic polymer substrates and it is expensive to produce large-scale and cost-effective sensors due to its complex process. In order to solve these problems, oxide piezoelectric films directly grown on flexible inorganic substrates in a simple and reliable way would be highly favored. Muscovite mica, $\text{KAl}_2(\text{AlSi}_3\text{O}_{10})\text{F}_2$, can serve as an ideal inorganic substrate for the fabrication of flexible oxide piezoelectric film sensors [27–32]. The advantages of muscovite mica substrate include its atomically smooth surface, high thermal stability ($\sim 1000^\circ\text{C}$) and mechanical flexibility. The monoclinic muscovite mica has a two-dimensional (2D) structure with an AlO_6 octahedral layer sandwiched by two $(\text{Si},\text{Al})\text{O}_4$ tetrahedral layers which are stacked further by a layer of potassium cations. This 2D layered material can be mechanically exfoliated like graphene down to few tens of micrometers. Furthermore, unlike the conventional rigid substrates, the crystalline structure of mica substrate allows the van der Waals (vdW) epitaxial growth of oxide films, reducing the substrate clamping effect and thus improving the physical properties [21,29].

For the first time, we report in this study that flexible PZT film is an excellent candidate for piezoelectric ultrasonic transducer used to receive Lamb wave for SHM of aircraft at *real-time*. High-quality epitaxial and flexible 500 nm PZT films were epitaxially grown on $\text{SrRuO}_3\text{--BaTiO}_3$ (SRO-BTO)-buffered mica substrates. Superiorly stable ferroelectricity and piezoelectricity can be maintained up to 250°C or bended up to 10^4 bending cycles under a radius of 8 mm. Based on experiment and simulation, by comparing the differences between the health response signals and damage response signals, we demonstrate that flexible PZT films can be used in *real-time* Lamb wave-based damage detection of both flat and curved aluminum plates, in comparison to the conventional PZT ceramics.

2. Experimental section

Film fabrication: Epitaxial $\text{Pb}(\text{Zr}_{0.53}\text{Ti}_{0.47})\text{O}_3$ (PZT) films were grown on mica substrates using pulsed laser deposition. During the deposition, the temperature was at 780°C and oxygen partial pressure was fixed at

0.25 mbar with a laser repetition rate of 4 Hz. Prior to the growth of PZT, BaTiO_3 buffer layer and SrRuO_3 electrode layer with a thickness of 30 nm and 33 nm were deposited at a substrate temperature of 750°C under an oxygen partial pressure of 0.2 mbar. After the deposition, the films were cooled at a slow rate of $3^\circ\text{C}/\text{min}$.

Basic characterization: The crystalline structure of thin films was investigated using high-resolution four circle X-ray diffraction (Panalytical Empyrean) and transmission electron microscopy (TEM, FEI Tecnai F20 analytical microscope). Piezoresponse force microscopy measurements were carried out by Asylum Research AFM MFP-3D origin. Ferroelectric performance was measured by a Radian Precision materials analyzer and the temperature was controlled by a Linkam Scientific Instruments HFS600E-PB4. Mechanical fatigue of the film was measured by a bending table (HEV-20). In order to conduct the Lamb wave-based damage detection on the aluminum plate, flexible PZT film was processed as a sensor. SrRuO_3 layer was used as the bottom electrode and top Au electrodes with an area of $7.065 \times 10^{-2} \text{ cm}^2$ were sputtered onto the flexible PZT film, forming a typical sandwich structure sensor. Indium was used to weld the film to the shielding wire and eventually to connect it to the measurement system which includes digital storage oscilloscope (Agilent MSOX 3014A), function generator (SDG 5122), power amplifier (KROHN-HITE MODEL 7602 M) and (homemade) charger amplifier were used.

Simulation: Commercial FEM software COMSOL Multiphysics 5.3a was adopted for its great advantages in solving the coupling of multiple physical fields. Fig. S2 shows the geometric model. The geometric size is the same with the experiment shown in Fig. 5a and summarized in Table S3. An adhesive layer is established between the sensor and the aluminum plate, and its thickness is 0.05 mm, which is close to the actual adhesive thickness. The material of the PZT ceramic is set as PZT 5A, in the COMSOL built-in material library, which is consistent with the material of the actual PZT ceramic ($\phi 8 \text{ mm} \times 0.48 \text{ mm}$, Fuji Ceramics Corporation). Because some of the parameters of the thin film material required for simulation cannot be measured by experiments, the material parameters of thin film here are set as PZT 6B [33], which is close to the flexible PZT film in structure and has similar element stoichiometric ratio and piezoelectric properties. The compliance coefficient, piezoelectric constant, and relative permittivity of the thin film are given according to formula (1) to (3) and the density of it is set as 7550 kg/m^3 . The material parameters of aluminum plate, mica, and adhesive layer are shown in Table S4. The lower surface of the piezoelectric chip and the film are grounded. A five-peak wave signal, given in formula (4), is applied to the upper surface of PZT. The amplitude A , frequency f , and peak number N are set as 70 V, 400 kHz and 5. The electric potential of the upper surface of the thin film is used as the Lamb wave response signal. The periphery of the aluminum plate is set as a weak boundary reflection. The free tetrahedral mesh is adopted in the mesh division.

$$s_E = \begin{bmatrix} 7.3496 & -1.9097 & -2.0024 & 0 & 0 & 0 \\ -1.9097 & 16.4 & -2.0024 & 0 & 0 & 0 \\ -2.0024 & -2.0024 & 7.6091 & 0 & 0 & 0 \\ 0 & 0 & 0 & 36.9 & 0 & 0 \\ 0 & 0 & 0 & 0 & 36.9 & 0 \\ 0 & 0 & 0 & 0 & 0 & 18.519 \end{bmatrix} \times 10^{-12} (\text{1 / Pa}) \quad (1)$$

$$d = \begin{bmatrix} 0 & 0 & 0 & 0 & 130 & 0 \\ 0 & 0 & 0 & 130 & 0 & 0 \\ -27 & -27 & 71 & 0 & 0 & 0 \end{bmatrix} \times 10^{-12} (\text{C / N}) \quad (2)$$

$$\epsilon_{rT} = \begin{bmatrix} 475 & 0 & 0 \\ 0 & 475 & 0 \\ 0 & 0 & 460 \end{bmatrix} \quad (3)$$

$$E = A \cdot [1 - \cos(2\pi ft / N)] \cdot \sin(2\pi ft) \cdot [t < (N / f)] \quad (4)$$

3. Results and discussion

PZT/SRO/BTO films with a 15 μm thick mica cleavage were exfoliated using a sharp blade, as illustrated in Fig. 1a. A typical X-ray diffraction (XRD) θ - 2θ scan of the PZT/SRO/BTO film reveals the observation of only (ll) PZT, SRO and BTO diffraction peaks with mica (00l), suggesting the epitaxial nature of thin films without other secondary phases (Fig. 1b). Due to the very weak interaction between the film and mica substrate through the vdW epitaxy, the strain caused by the lattice mismatch between the film and mica substrate is fully relaxed. This is confirmed by X-ray reciprocal space map (RSM) (Fig. 1c). Furthermore, the phi-scan of PZT (330), SRO (330), BTO (330) and mica (690) reflections were used to determine the in-plane structural relationships (Fig. 1d). The six-fold symmetry of PZT (330), SRO (330) and BTO (330) could be explained by the formation of multi-domains [21]. The detailed microstructure of the PZT/SRO/BTO film was further investigated by transmission electron microscope (TEM) and selected area electron diffraction (SAED) as shown in Fig. 1e–h. Low-magnification TEM image (Fig. 1e) reveals the layer structure of the PZT/SRO/BTO/mica. High-magnification TEM images (Fig. 1f and g) and

exhibit the defect-free and coherent interfaces at the interfaces of PZT/SRO and SRO/BTO/mica in the heterostructure. Based on the results of XRD and TEM, high-quality heteroepitaxy of PZT/SRO/BTO films on flexible inorganic mica substrates is delivered.

To investigate the bending effect on the stability of ferroelectric and piezoelectric properties, mechanical stretching was applied and a sketch is shown in Fig. 2a. Ferroelectric hysteresis loops, obtained before and after bending 10^4 cycles under a radius of 8 mm, are displayed in Fig. 2b. It can be seen that the ferroelectric properties of flexible PZT films are not affected by mechanical fatigue. Moreover, as shown in Fig. S1, robust ferroelectric hysteresis loops were measured from room temperature to 250 °C, indicating the ferroelectricity can be retained in flexible PZT films by at least 250 °C. Piezoelectric properties were further studied by piezoelectric force microscope (PFM) and the results are shown in Fig. 2c and d. An outstanding stability of piezoelectricity is also observed after bending 10^4 cycles under a radius of 8 mm. In comparison to PZT films grown on the conventional rigid substrates [34–36], flexible PZT films grown on organic substrates and metal foils and flexible PZT-based composites (Table S2), an enhanced piezoelectric performance, such as a d_{33} of around 130 p.m. V^{-1} and no poling

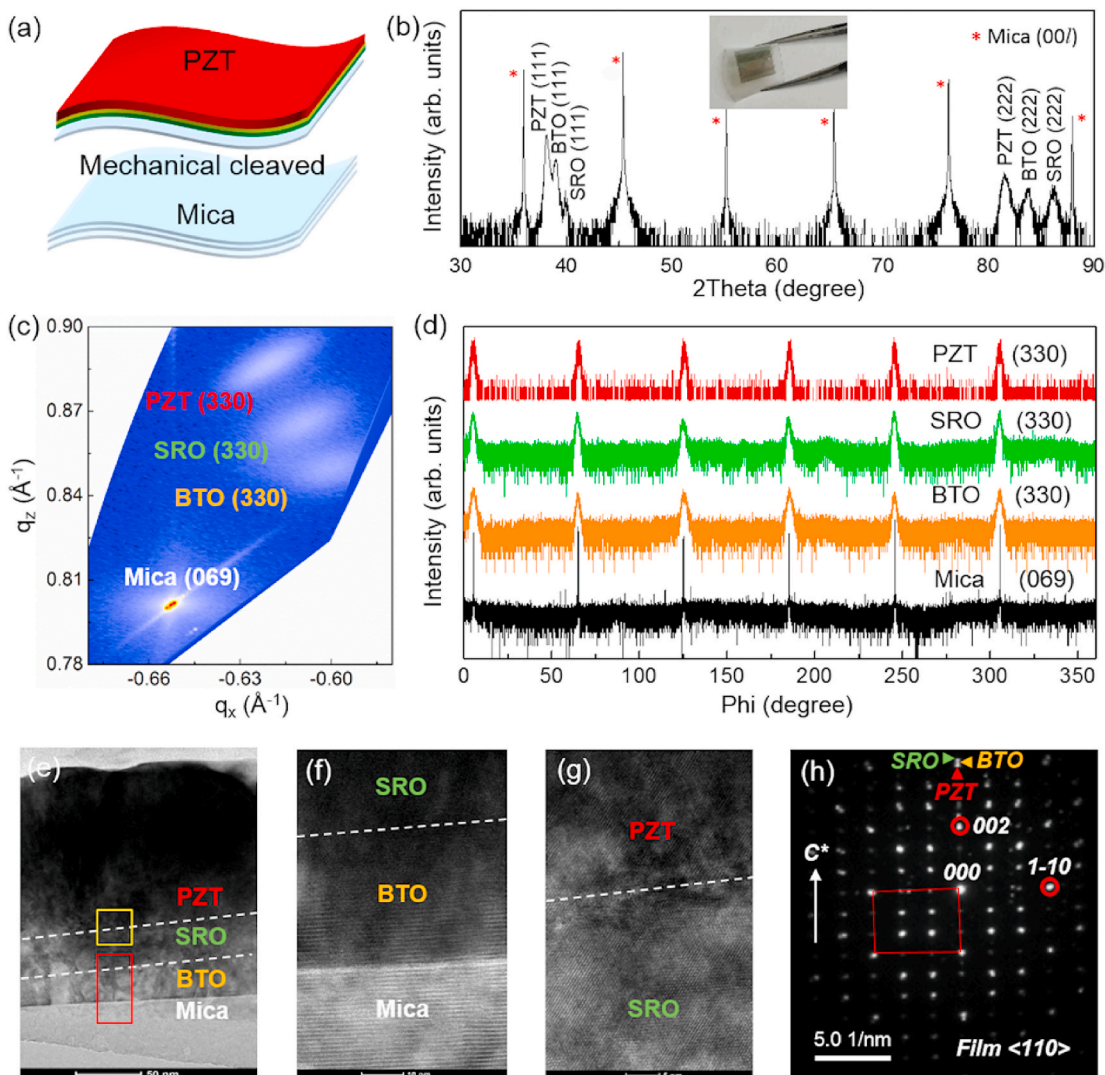


Fig. 1. (A) Schematic illustration of mechanical exfoliation of PZT/SRO/BTO/mica. (b) A typical XRD θ - 2θ scan of PZT/SRO/BTO/mica film. The inset shows a photograph of the film with bending. (c) Reciprocal space map of (069) and (330) Brag reflections of mica and PZT/SRO/BTO, respectively. (d) Phi-scans of PZT (330), SRO (330), BTO (330) and mica (069). (e) TEM image showing the PZT/SRO/BTO layers and mica substrate. (f) HRTEM image of the BTO and mica interface and the SRO and BTO interface, corresponding to the red box in e. (g) HRTEM image of the PZT and SRO interface, corresponding to the yellow box in e. (h) SAED pattern indicating the high quality epitaxial PZT/SRO/BTO film grown on mica.

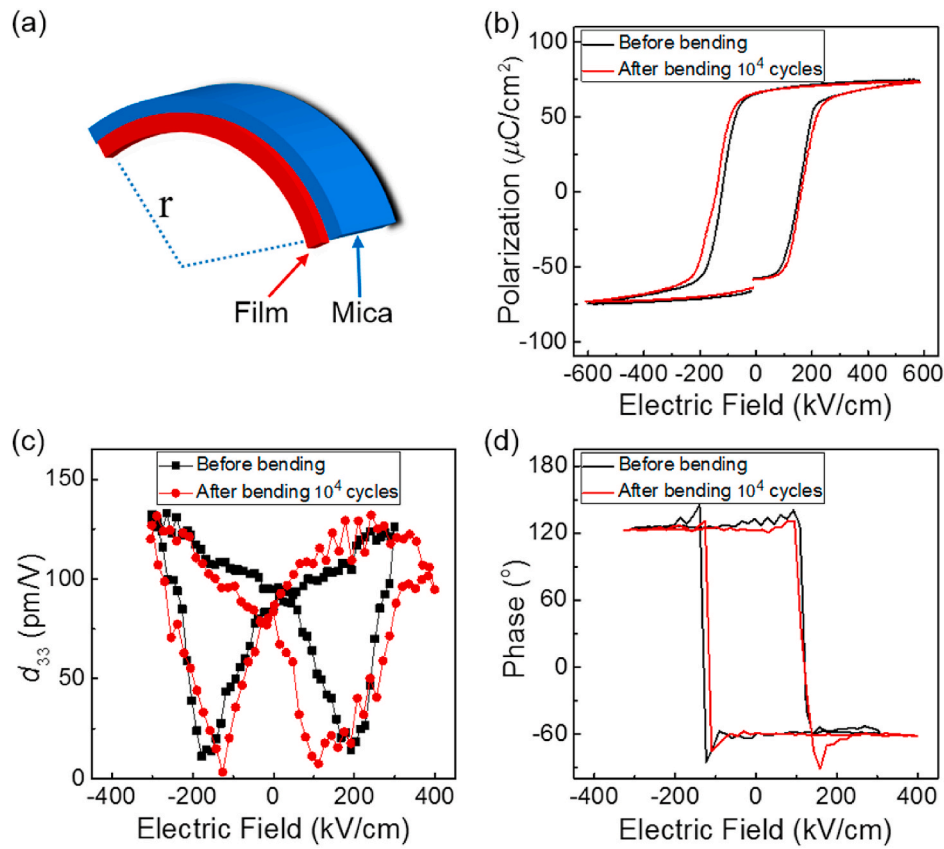


Fig. 2. (A) A sketch of mechanical bending. (b) P-E hysteresis loops, (c) piezoelectric coefficient d_{33} and (d) phase of the PZT/SRO/BTO film before and after bending by the radius of 8 mm and 10⁴ cycles.

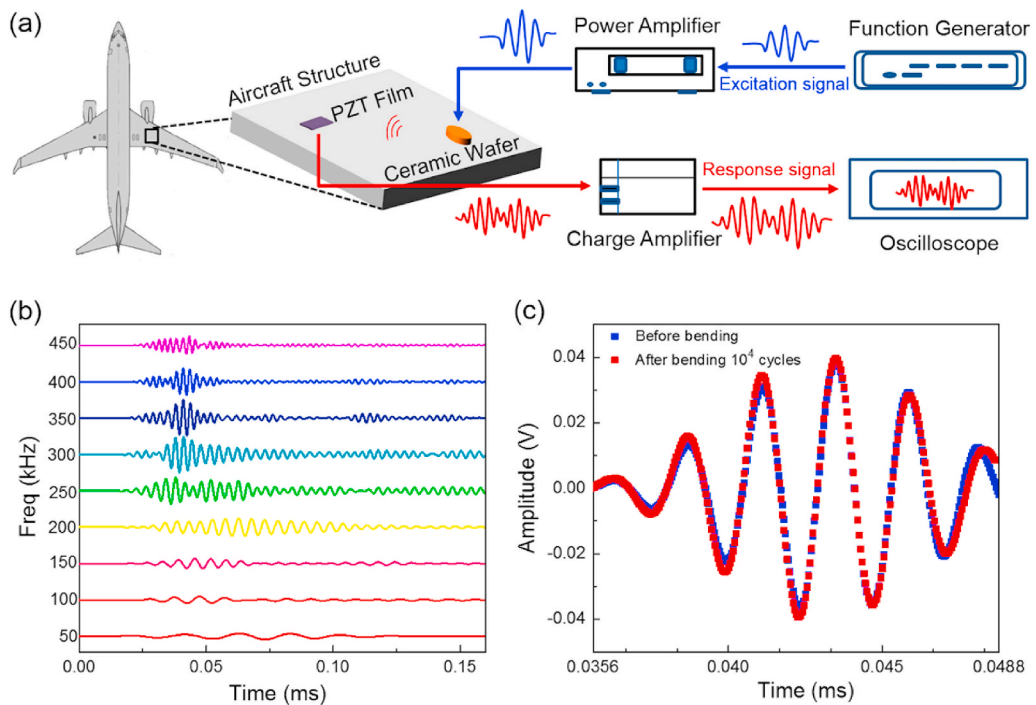


Fig. 3. (A) Schematic diagram of the experimental setup for measuring Lamb wave response signal. (b) Lamb wave response signals at different central frequencies obtained from the aluminum flat-plate. (c) S₀ mode of Lamb wave response signals at a central frequency of 400 kHz before and after bending by the radius of 8 mm and 10⁴ cycles.

process, is achieved. The improved piezoelectric performance of flexible PZT films could be attributed to crystalline feature (weak vdW interaction at the inter-layer) of mica substrate for achieving vdW epitaxial growth [37,38].

Lamb wave was firstly proposed by Horace Lamb in 1917 and is a kind of elastic disturbance propagating in solid plate structure with free boundary [39]. Lamb wave can be excited by applying a specific wave form to the piezoelectric element arranged on the plate structure. Generally, Lamb wave excited by excitation should be sensitive to the damaged structure, which can be easily identified from the differences of Lamb wave before and after the damage event [40–42]. Commonly-used excitation signals include broadband frequency excitation signal, narrowband frequency excitation signal and single frequency excitation signal. Narrowband signal has short duration in time domain and narrow spectrum width which is widely used in relevant research and application [43]. The mechanical modeling method of metal material structure, like aluminum, is simple and accurate. Also, aluminum material is one of the materials widely used in aircraft structure at present. Therefore, an aluminum plate was taken as the research object for exploring the flexible PZT film sensor for the Lamb wave-based damage monitoring. Fig. 3a shows an enlarged schematic diagram of the aircraft for SHM. PZT ceramic ($\phi 8 \text{ mm} \times 0.48 \text{ mm}$, Fuji Ceramics Corporation) and flexible PZT film ($10 \text{ mm} \times 5 \text{ mm} \times 500 \text{ nm}$) were pasted on an aluminum flat-plate with a thickness of 2 mm as actuating element and sensing element, respectively. The distance between PZT ceramic and flexible PZT film is set to 15 cm. A function generator is used to generate a five-peak wave signal with different central frequencies, which is amplified to $\pm 70 \text{ V}$ by a power amplifier and applied to the PZT ceramic. Based on the inverse piezoelectric effect, the deformation of PZT ceramic causes the Lamb wave to be excited and propagated on the aluminum flat-plate. The flexible PZT film, due to the positive piezoelectric effect, will convert the deformation induced by Lamb wave into electrical signals which are amplified by a charge amplifier and finally displayed on an oscilloscope (Fig. 3a). Fig. 3b shows the cascade diagram of Lamb wave response signal obtained by sweeping the frequencies. Each line represents a response signal at a central frequency ranging from 50 kHz to 450 kHz. Theoretically, with the increase of the central frequency of the excitation signal, the speed of S_0 mode of the response signal becomes slower [41]. The amplitude and waveform of Lamb wave with a frequency of 400 kHz are the most stable and the effect of boundary scattering is minimal. Thus, the S_0 mode of Lamb wave of 400 kHz is selected for subsequent damage detection experiments. As discussed above, we have proven that mechanical bending has negligible influence on the piezoelectric and ferroelectric

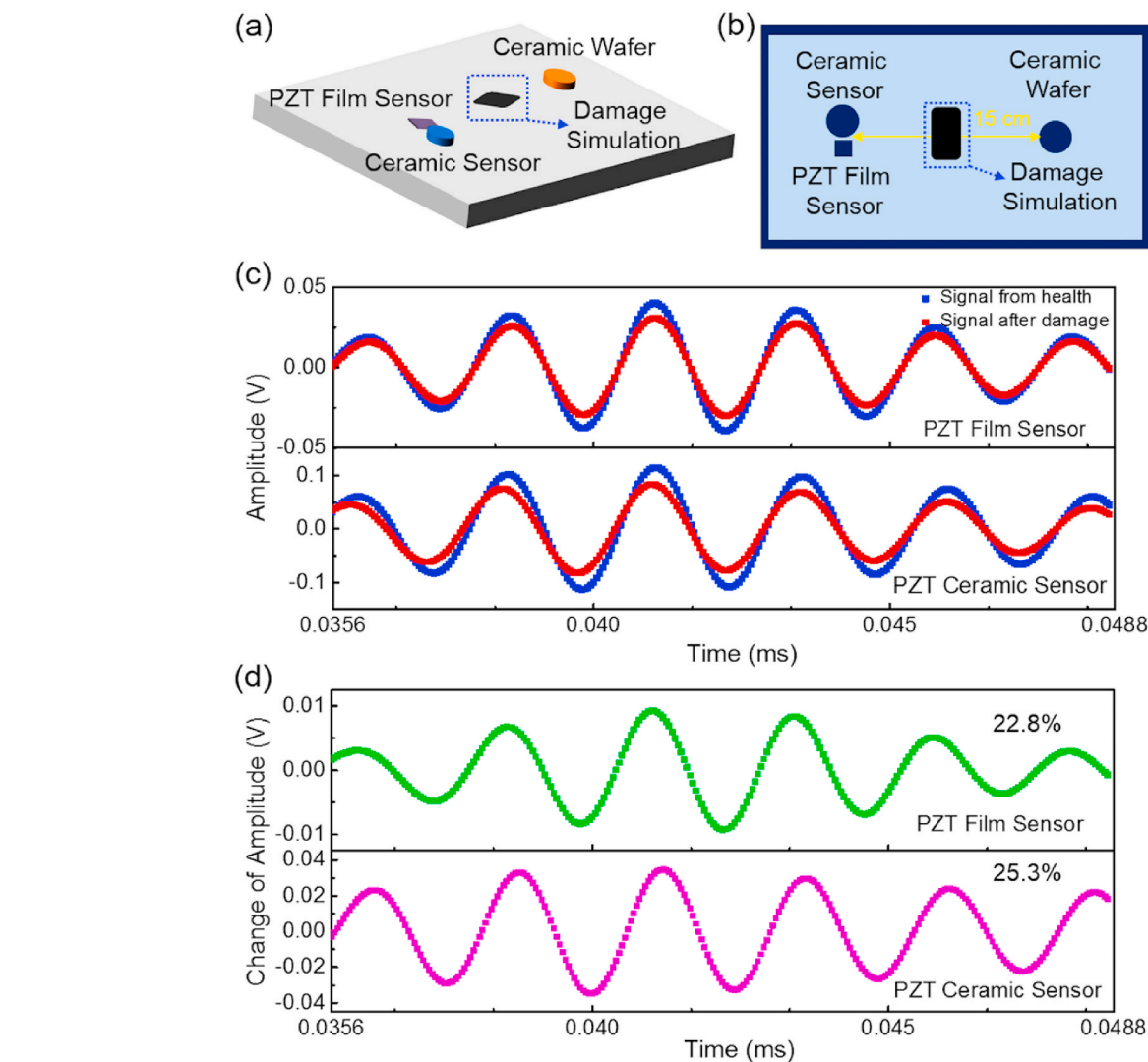


Fig. 4. (A) Schematic diagram of detecting damage on the aluminum flat-plate. (B) Top-view of the schematic diagram in a. (C) S_0 mode of Lamb wave response signals in S_0 mode at a central frequency of 400 kHz obtained from the flexible PZT film (top panel) and the PZT ceramic (bottom panel) sensors. (D) Change of amplitude of Lamb wave response signals in S_0 mode for the flexible PZT film (top panel) and the PZT ceramic (bottom panel) sensors obtained from (C).

properties of the flexible PZT film. Fig. 3c shows the S_0 mode of Lamb wave response signals before and after bending 10^4 cycles under a radius of 8 mm. We can clearly see that the amplitude and waveform of the Lamb wave response signals are almost the same before and after bending.

The conception of Lamb wave-based damage detection is based on the differences of Lamb wave response signals before and after the damage event. Once the damage occurs, the amplitudes of Lamb wave response signals will attenuate obviously [44,45]. Fig. 4a shows a typical schematic diagram of an experimental system for Lamb wave-based damage monitoring system. The top view is shown in Fig. 4b. On the right, one PZT ceramic wafer is adopted as the excitation source. On the left, another PZT ceramic wafer and flexible PZT film are adopted as sensing elements. The distance between sensing elements and excitation source is still kept at 15 cm. Artificial damage case is bonded on the aluminum plate to simulate the real damage. Fig. 4c displays the Lamb wave response signals obtained by the flexible PZT film and the PZT ceramic, before and after the damage event. The response signal received by the flexible PZT film is amplified by 50 times through the charge amplifier. We noticed that the S_0 modes of Lamb wave response signals received by PZT ceramic and flexible PZT film sensors are basically consistent, except for the difference in signal amplitude, which is due to the difference of their piezoelectric properties. On the other hand, after the damage event, the amplitude of Lamb wave response signal detected by flexible PZT film is significantly weaker than that of health Lamb wave response signal. The change of amplitude of response signals before and after the damage event is shown in Fig. 4d. We calculated that the average amplitude of six peaks of response signals after the damage event received by flexible PZT film and PZT ceramic sensors are decreased by 22.8% and 25.3%, respectively. This further suggests that the sensitivity of flexible PZT film sensor is at same level as that of the PZT ceramic sensor. These results demonstrate that flexible PZT film sensor may replace the role of PZT ceramic sensor in Lamb wave-based damage detection. It should be also emphasized that flexible PZT film is ultra-thin, soft and light-weight, which can be directly mounted on the surface of the specimen without affecting its shape and mechanical motion.

It is well known that, aircraft structures often contain complex components with curved surfaces in addition to the flat components. The thickness, weight and rigidity of conventional PZT ceramics limit their damage monitoring ability on these complex components with curved surfaces. Flexible PZT film can overcome this disadvantage of PZT ceramic. As shown in Fig. 5a and b, flexible PZT film is mounted on the curved part of aluminum plate, while PZT ceramic as excitation source is attached to the flat part of aluminum plate. The distance between PZT

ceramic and flexible PZT film sensor is still 15 cm. The integration of flexible PZT film and the curved surface aluminum plate realize the propagation of Lamb wave on the curved part of the aluminum plate, which is difficult for PZT ceramic or rigid piezoelectric film. Similarly, artificial damage case is bonded on the aluminum plate to simulate the real damage, and Lamb wave response signals were acquired before and after the damage simulation. From Fig. 5c, we can see that the amplitudes of Lamb wave response signals are significantly decreased after the damage simulation.

In order to further verify the correctness of Lamb wave response signals of flexible PZT film on the curved aluminum plate, the finite element simulation (FEM) analysis of the PZT thin film on the aluminum plate was carried out. The details are provided in the experiment section. Dynamic Lamb waves excited at 0.02 ms and received at 0.05 ms are shown in Fig. 6a and b, respectively. It can be seen that Lamb waves are indeed transferred through the curved surface and received by flexible PZT film. The Lamb wave response signals obtained from experiment and simulation are plotted together (Fig. 6c). The response signals are normalized by amplitude and aligned by the peak value for easy comparison. Obviously, the S_0 mode of the simulation signal is in good agreement with that of the experiment signal, which verifies the correctness of the experiment signal. These results strongly suggest that flexible PZT film sensor can achieve the damage monitoring on the curved aluminum plate.

4. Conclusion

In summary, we have fabricated the high-quality epitaxial and flexible PZT films on SRO-BTO-buffered inorganic mica substrates by pulsed laser deposition, and further demonstrated its utilization as an ultrasonic sensor in Lamb wave-based SHM of aircraft. The piezoelectric coefficient (d_{33}) with a value of ~ 130 p.m. V^{-1} is obtained in flexible PZT film. The value is higher than that of PZT films grown on the conventional rigid substrates, organic polymer substrates and metal foils. Furthermore, an outstanding stability of ferroelectric and piezoelectric properties is demonstrated by bending 10^4 cycles under a radius of 8 mm. Proven by experiment and simulation, Lamb wave-based damage monitoring on both flat and curved aluminum plate was demonstrated by flexible PZT film sensor. Further, the sensitivity is same as that of conventional PZT ceramics. Our work demonstrates the feasibility to apply flexible PZT films for light-weight and high-density integrated receiver sensors for the *real-time* SHM of aging aircraft.

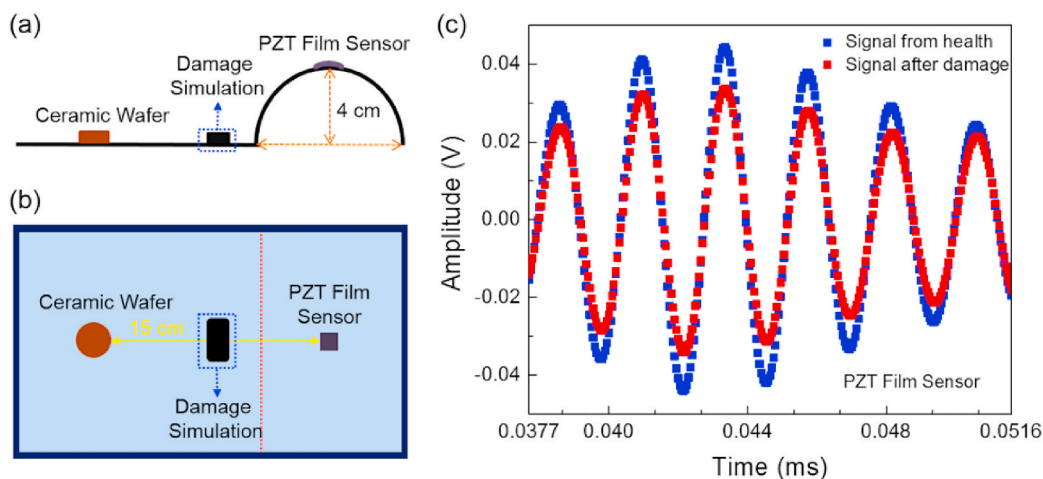


Fig. 5. (A) Cross-sectional view of schematic diagram of detecting damage on the curved aluminum plate. (B) Top-view of the schematic diagram in a. (C) S_0 mode of Lamb wave response signal at a central frequency of 400 kHz obtained from the flexible PZT film.

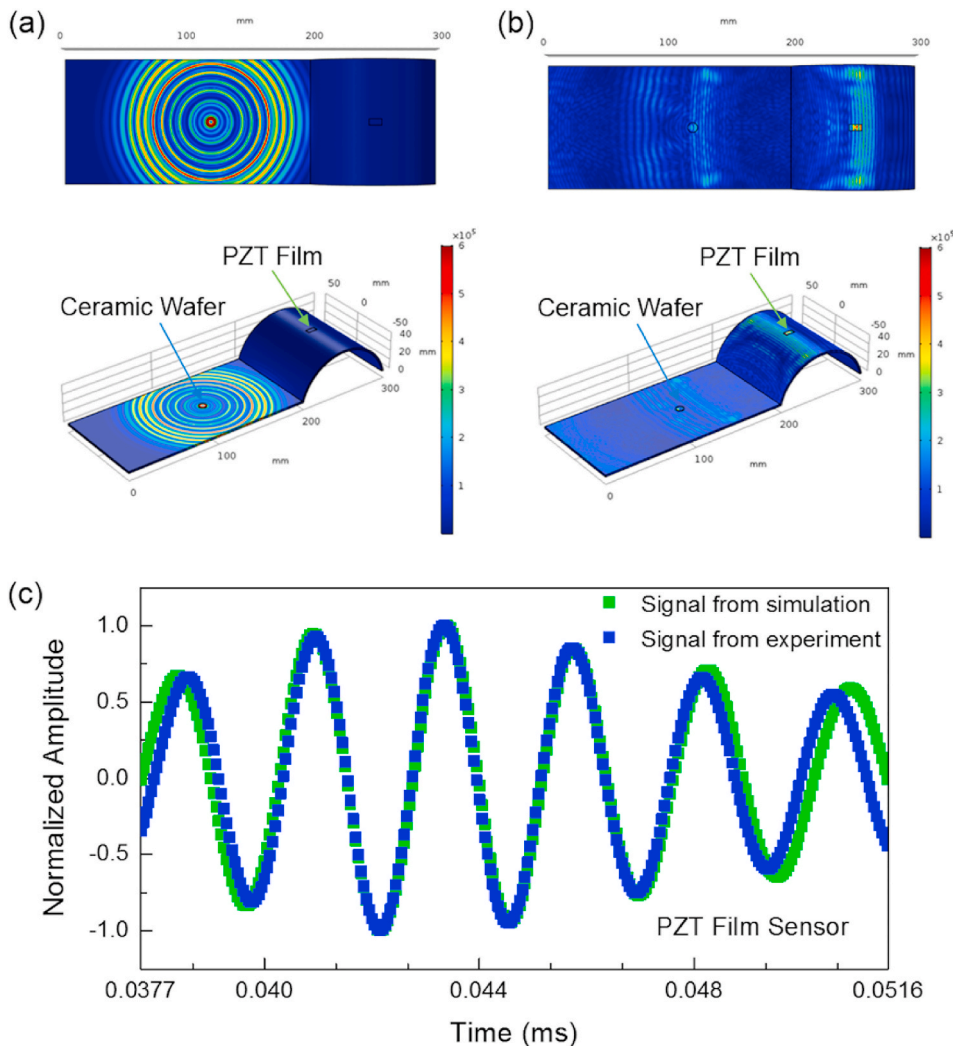


Fig. 6. Dynamic Lamb waves (a) excited at 0.02 ms under top view (top panel) and side view (bottom panel) and (b) received at 0.05 ms under top view (top panel) and side view (bottom panel). (c) Comparison of S_0 mode of Lamb wave response signals at a central frequency of 400 kHz obtained from the simulation and experiment.

Author contribution

X.Z and Y.W contributed equally to this work. H.Y, W.-W.L and L.Q. supervise the project. X. Z fabricated the samples and carried out XRD, piezoelectric and ferroelectric measurements with the support from X. S, M.L, Y. J, F. Q and J.F. Y.W and L.Q. carried out the measurement and the simulation of SHM system. J.J, X. W and H.W performed the STEM measurements. X. Z, W.-W.L and H.Y prepared the manuscript with the contribution from all authors.

Declaration of competing interest

The authors declare that they have no known competing financial interests or personal relationships that could have appeared to influence the work reported in this paper.

Acknowledgements

This work was supported by National Natural Science Foundation of China of China (Grant No.U1632122, 11774172, 51635007 and 51602152), China Scholarship Council (File No.201906830034), Open Fund of Key Laboratory for Intelligent Nano Materials and Devices of the Ministry of Education (INMD-2019M06). X.W., J.J., and H.W.

acknowledge the support from the U.S. National Science Foundation (DMR-1565822 and 1809520) for the high resolution TEM and STEM effort.

Appendix A. Supplementary data

Supplementary data to this article can be found online at <https://doi.org/10.1016/j.ceramint.2021.01.180>.

References

- [1] J.B. Ihn, F.K. Chang, Pitch-catch active sensing methods in structural health monitoring for aircraft structures, *Struct. Health Monit.* 7 (2008) 5–19.
- [2] P.D. Foote, Integration of structural health monitoring sensors with aerospace, composite materials and structures, *Mater. Werkst.* 46 (2015) 197–203.
- [3] S. Yuan, Y. Ren, L. Qiu, H. Mei, A multi-response-based wireless impact monitoring network for aircraft composite structures, *IEEE Trans. Ind. Electron.* 63 (2016) 7712–7722.
- [4] X. Qing, W. Li, Y. Wang, H. Sun, Piezoelectric transducer-based structural health monitoring for aircraft applications, *Sensors* 19 (2019) 545–572.
- [5] M.S. Salmanpour, Z. Sharif Khodaei, M.H. Aliabadi, Impact damage localisation with piezoelectric sensors under operational and environmental conditions, *Sensors* 17 (2017) 1178–1196.
- [6] W. Harizi, S. Chaki, G. Bourse, M. Ourak, Mechanical damage characterization of glass fiber-reinforced polymer laminates by ultrasonic maps, *Compos. B Eng.* 70 (2015) 131–137.

[7] S. Boccardi, G.M. Carloni, G. Meola, P. Russo, G. Simeoli, Evaluation of polypropylene based composites from thermal effect developing under cyclic bending tests, *Compos. Struct.* 182 (2017) 628–635.

[8] A. Katunin, K. Dragan, M. Dziendzikowski, Damage identification in aircraft composite structures: a case study using various non-destructive testing techniques, *Compos. Struct.* 127 (2015) 1–9.

[9] J. Dong, A. Locquet, N.F. Declercq, D.S. Citrin, Polarization-resolved terahertz imaging of intra-and inter-laminar damages in hybrid fiber-reinforced composite laminate subject to low-velocity impact, *Part. B-Eng.* 92 (2016) 167–174.

[10] S.S. Kessler, S.M. Spearing, C. Soutis, Damage detection in composite materials using Lamb wave methods, *Smart Mater. Struct.* 11 (2002) 269–278.

[11] S.M. Yang, C.C. Hung, K.H. Chen, Design and fabrication of a smart layer module in composite laminated structures, *Smart Mater. Struct.* 14 (2005) 315–320.

[12] L. Qiu, B. Liu, S. Yuan, Z. Su, Impact imaging of aircraft composite structure based on a model-independent spatial-wave number filter, *Ultrasonics* 64 (2016) 10–24.

[13] R. Lammering, U. Gabbert, M. Sinapius, T. Schuster, P. Wierach, *Lamb-wave Based Structural Health Monitoring in Polymer Composites*, Springer, 2017.

[14] J. Wu, S. Yuan, S. Ji, G. Zhou, Y. Wang, Z. Wang, Multi-agent system design and evaluation for collaborative wireless sensor network in large structure health monitoring, *Expert Syst. Appl.* 37 (2010) 2028–2036.

[15] C. Tuloup, W. Harizi, Z. Aboura, Y. Meyer, K. Khellil, R. Lachat, On the manufacturing, integration, and wiring techniques of in situ piezoelectric devices for the manufacturing and structural health monitoring of polymer–matrix composites: a literature review, *J. Intell. Mater. Syst. Struct.* 30 (2019) 2351–2381.

[16] D.H. Wang, S.L. Huang, Health monitoring and diagnosis for flexible structures with PVDF piezoelectric film sensor array, *J. Intell. Mater. Syst. Struct.* 11 (2000) 482–491.

[17] H. Luo, S. Hanagud, PVDF film sensor and its applications in damage detection, *J. Aerospace Eng.* 12 (1999) 23–30.

[18] B. Ren, C.J. Lissenden, PVDF multielement Lamb wave sensor for structural health monitoring, *IEEE T. Ultrason. Ferr.* 63 (2016) 178–185.

[19] H.I. Schlaberg, J.S. Duffy, Piezoelectric polymer composite arrays for ultrasonic medical imaging applications, *Sensor Actuat. A-Phys* 44 (1994) 111–117.

[20] K.I. Park, S. Xu, Y. Liu, G.T. Hwang, S. Kang, Z.L. Wang, K.J. Lee, Piezoelectric BaTiO₃ thin film nanogenerator on plastic substrates, *Nano Lett.* 10 (2010) 4939–4943.

[21] Y.H. Do, M.G. Kang, J.S. Kim, C.Y. Kang, S.J. Yoon, Fabrication of flexible device based on PAN-PZT thin films by laser lift-off process, *Sensor Actuat. A-Phys.* 184 (2012) 124–127.

[22] Z.W. Yin, H.S. Luo, P.C. Wang, G.S. Xu, Growth, characterization and properties of relaxor ferroelectric PMN-PT single crystals, *Ferroelectrics* 229 (1999) 207–216.

[23] Z. Wang, Q.T. Xue, Y.Q. Chen, Y. Shu, H. Tian, Y. Yang, D. Xie, J.W. Luo, T.L. Ren, A flexible ultrasound transducer array with micro-machined bulk PZT, *Sensors* 15 (2015) 2538–2547.

[24] R. Hou, Y.Q. Fu, D. Hutson, C. Zhao, E. Gimenez, K.J. Kirk, Use of sputtered zinc oxide film on aluminium foil substrate to produce a flexible and low profile ultrasonic transducer, *Ultrasonics* 68 (2016) 54–60.

[25] M. Safaei, H.A. Sodano, S.R. Anton, A review of energy harvesting using piezoelectric materials: state-of-the-art a decade later (2008–2018), *Smart Mater. Struct.* 28 (2019) 113001–113063.

[26] Y.Q. Fu, J.K. Luo, N.T. Nguyen, A.J. Walton, A.J. Flewitt, X.T. Zu, Y. Li, G. McHale, A. Matthews, E. Iborra, H. Du, W.I. Milne, Advances in piezoelectric thin films for acoustic biosensors, acoustofluidics and lab-on-chip applications, *Prog. Mater. Sci.* 89 (2017) 31–91.

[27] J. Jiang, Y. Bitla, C. Huang, T. Do, H. Liu, Y. Hsieh, C. Ma, C. Jang, Y. Lai, P. Chiu, W. Wu, Y. Chen, Y. Zhou, Y. Chu, Flexible ferroelectric element based on van der Waals heteroepitaxy, *Sci. Adv.* 3 (2017) 1700121–1700128.

[28] Y. Yang, G. Yuan, Z. Yan, Y. Wang, X. Lu, J.M. Liu, Flexible, semitransparent, and inorganic resistive memory based on BaTi_{0.95}Co_{0.05}O₃ Film, *Adv. Mater.* 29 (2017) 1700425–1700426.

[29] T. Amrillah, Y. Bitla, K. Shin, T. Yang, Y. Hsieh, Y. Chiou, H. Liu, T. Do, D. Su, Y. Chen, S. Jen, L. Chen, K. Kim, J. Juang, Y. Chu, Flexible multiferroic bulk heterojunction with giant magnetoelectric coupling via van der Waals epitaxy, *ACS Nano* 11 (2017) 6122–6130.

[30] M. Tsai, J. Jiang, P. Shao, Y. Lai, J. Chen, S. Ho, Y. Chen, D. Tsai, Y. Chu, Oxide heteroepitaxy-based flexible ferroelectric transistor, *ACS Appl. Mater. Interfaces* 11 (2019) 25882–25890.

[31] H. Liu, C. Wang, D. Su, T. Amrillah, Y. Hsieh, K. Wu, Y. Chen, J. Juang, L. Eng, S. Jen, Y. Chu, Flexible heteroepitaxy of CoFe₂O₄/muscovite bimorph with large magnetostriction, *ACS Appl. Mater. Interfaces* 9 (2017) 7297–7304.

[32] C. Ren, C. Tan, L. Gong, M. Tang, M. Liao, Y. Tang, X. Zhong, H. Guo, J. Wang, Highly transparent, all-oxide, heteroepitaxy ferroelectric thin film for flexible electronic devices, *Appl. Surf. Sci.* 458 (2018) 540–545.

[33] H. Lee, E. Guo, J. Kwak, S. Hwang, K. Dörr, J. Lee, J. Young Jo, Controllable piezoelectricity of Pb(Zr_{0.2}Ti_{0.8})O₃ film via in situ misfit strain, *Appl. Phys. Lett.* 110 (2017), 032901–032905.

[34] D. Taylor, D. Damjanovic, Piezoelectric properties of rhombohedral Pb(Zr, Ti)O₃ thin films with (100), (111), and “random” crystallographic orientation, *Appl. Phys. Lett.* 76 (2000) 1615–1617.

[35] V. Nagarajan, A. Roytburd, A. Stanishevsky, S. Prasertchoung, T. Zhao, L. Chen, J. Melngailis, O. Auciello, R. Ramesh, Dynamics of ferroelastic domains in ferroelectric thin films, *Nat. Mater.* 2 (2003) 43–47.

[36] Y. Celik, E. Flahaut, E. Suvaci, A comparative study on few-layer graphene production by exfoliation of different starting materials in a low boiling point solvent, *FlatChem* 1 (2017) 74–88.

[37] W. Gao, L. You, Y. Wang, G. Yuan, Y. Chu, Z. Liu, J. Liu, Flexible PbZr_{0.52}Ti_{0.48}O₃ capacitors with giant piezoelectric response and dielectric tunability, *Adv. Elec. Mater.* 3 (2017) 1600542–1600546.

[38] H. Lamb, On waves in an elastic plate, *Proc. R. Soc. A93* (1917) 114–128.

[39] R.L. Clark, M.R. Flemming, C.R. Fuller, Piezoceramic actuators for distributed vibration excitation of thin plates, *J. Vib. Acoust.* 115 (1993) 332–339.

[40] Z. Su, L. Ye, Y. Lu, Guided Lamb waves for identification of damage in composite structures: a review, *J. Sound Vib.* 395 (2006) 753–780.

[41] R.A. Badcock, E.A. Birt, The use of 0-3 piezocomposite embedded Lamb wave sensors for detection of damage in advanced fibre composites, *Smart Mater. Struct.* 9 (2000) 291–297.

[42] V. Giurgiutiu, Tuned Lamb wave excitation and detection with piezoelectric wafer active sensors for structural health monitoring, *J. Intell. Mater. Syst. Struct.* 16 (2005) 291–305.

[43] K. Worden, S.G. Pierce, G. Manson, W.R. Philp, W.J. Staszewski, B. Culshaw, Detection of defects in composite plates using Lamb waves and novelty detection, *Int. J. Syst. Sci.* 31 (2000) 1397–1409.

[44] M. Lemistre, D. Balageas, Structural health monitoring system based on diffracted Lamb wave analysis by multiresolution processing, *Smart Mater. Struct.* 10 (2001) 504–511.

[45] D. Berlincourt, *Piezoelectric Crystals and Ceramics, Ultrasonic Transducer Materials*, Springer, Boston MA, 1971, pp. 63–124.